doi:10.7289/V5TX3C9K

GSICS Quarterly

Global Space-based Inter-Calibration System

CMA • CNES • EUMETSAT • JMA • KMA • NASA • NIST • NOAA • WMO

http://gsics.wmo.int

Vol. 3, No. 2, 2009

Dr. Robert A. Iacovazzi, Jr., Editor

SPECIAL ISSUE

Estimating Uncertainties of GSICS Satellite Inter-comparison Results

As GSICS international research collaboration matures, some focus has shifted from how to inter-compare satellite instruments to how to distribute inter-comparison results. One decision made at the most recent Joint GSICS Research and Data Working Group meeting, held in January 2009 at JMA Headquarters in Tokyo, is for GSICS researchers to develop correction coefficients for each satellite instrument data set that will adjust those data to a state-of-the-art, on-orbit reference standard. In doing so, it has become the responsibility of GSICS researchers to also estimate the uncertainties associated with those correction coefficients. This Special Issue of *GSICS Quarterly* includes articles focusing on GSICS members' recent progress towards defining these uncertainties.

Coalescing GSICS Correction Coefficients

In this article, we would like to present a technique to adjust the uncertainty estimates of each point in a time series, so that the variance of the time series is consistent with the uncertainty estimates of its component points. This technique can be used, for example, to combine the coefficients of a GSICS correction. All data, together with their uncertainties, should be propagated along a model according to the rules laid out by the Guide to the Expression of Uncertainty in Measurement (GUM) by Bureau International de Poids et Mesures (BIPM 1993).

The basis of the evaluation is existing data x_i with an associated standard uncertainty $u(x_i)$. If we assume that $u(x_i)$ is independent of time and location, the arithmetic (or weighted) mean is the best way to combine the data (Draper *et al.*, 1981). Because this is a linear problem, we do not distinguish between measurement model and the equation for the expectation value y. So we use

$$y = \frac{1}{n} \cdot \sum_{i=1}^{n} (x_i + \delta x_i) \,, \qquad (1)$$

with n being the number of data x_i. Initially, all δx_i are set to zero. Under the assumption that the data values x_i are not correlated, the uncertainty $u(y)$ associated with the expectation value y can be calculated with

$$u(y) = \frac{1}{n} \cdot \sqrt{\sum_{i=1}^{n} u^2(x_i) + \sum_{i=1}^{n} u^2(\delta x_i)} \,. \qquad (2)$$

Unfortunately, the values x_i are often correlated because of common elements in their evaluation models. In these cases it is practical to separate the common correlated uncertainty components from the uncorrelated uncertainty component and propagate only the uncorrelated part. The correlated part can be simply added at the end.

As can be seen from Equation 2, the actual spread of values does not influence the uncertainty of the average. This would be correct if the spread of values is small enough, but we would miss something when the spread is too large. What we need is a test to determine if the actual spread is sufficiently small and a way to cope with it in case it is not.

We suggest a metrological consistency test as proposed in Datla *et al.* (2009). We calculate the difference ε_i as

$$\varepsilon_i = (x_i + \delta x_i) - y \,. \qquad (3)$$

The uncertainty associated with ε_i is

$$u^2(\varepsilon_i) = \frac{1}{n^2} \left[\begin{array}{c} (n-1)^2 u^2(x_i) + \sum_{j \neq i} u^2(x_j) \\ + (n-1)^2 u^2(\delta x_i) + \sum_{j \neq i} u^2(\delta x_j) \end{array} \right] . \qquad (4)$$

Two values are consistent if the absolute value of the difference ε_i between the values is smaller than a multiple k of the uncertainty of that difference, or

$$|\varepsilon_i| \leq k \cdot u(\varepsilon_i) \,. \qquad (5)$$

Usually k is set to 2.0. The spread of values is small enough if the average value y is consistent with the contributing values $x_i + \delta x$.

When all values fulfil the criterion in Equation 5, then the values and their uncertainties are consistent. In case one of the differences fails the test, we need to introduce uncertainty

components for δx_i to handle the inconsistency and recalculate Equations 1 to 4. If the number of data values n is large (>20), it is possible to weaken the criterion by choosing a larger k or allowing some data not to satisfy Equation 5.

As far as additional information is available, we can use it to establish a reasonable uncertainty $u(\delta x_i)$. If we have no basis to judge the uncertainty of the results $x_1,\ldots, x_n$, it is reasonable to assign the same standard uncertainty to all the deviations δx_i.

$$\delta x_i = 0, \quad u(\delta x_i) = u(\delta x), \quad i = 1 \ldots n \,. \tag{6}$$

Combining Equation 4 and Equation 6 we have

$$u(\varepsilon_i) = \frac{1}{n} \cdot \sqrt{\begin{matrix}\left(n^2 - n\right) \cdot u^2(\delta x) \\ +\left(n-1\right)^2 u^2(x_i) + \sum_{j \neq i} u^2(x_j)\end{matrix}} \,. \tag{7}$$

The minimum value for $u(\delta x)$ to obtain consistency is

$$u(\delta x) \geq \max\left\{u_{\mathrm{ex},i}, i = 1 \ldots n\right\} \tag{8}$$

with

$$u_{\mathrm{ex},i} = \sqrt{\frac{n}{n-1}\left[\left(\frac{x_i - y}{k}\right)^2 - \frac{1}{n^2} \cdot \left(\begin{matrix}\left(n-1\right)^2 u^2(x_i) \\ +\sum_{j \neq i} u^2(x_j)\end{matrix}\right)\right]} \,. \tag{9}$$

In the absence of additional knowledge we can use the lower bound uncertainty given by Equation 8.

In practice, it is useful to define a ζ-function as

$$\zeta(x) = \frac{|x|}{u(x)}, \quad u(x) \neq 0 \,. \tag{10}$$

The ζ-function is used in Figure 1 to show inconsistencies in a small subset of data. Any values that exceed the given limit of 2.0 show inconsistencies. The diagram allows an easy judgment whether the data and their uncertainties are consistent.

The following algorithm can be used to implement the consistency check in practice.

1. Calculate all data x_i and the uncertainties $u(x_i)$.
2. Calculate the average y (Equation 1).
3. Set $u(\delta x) = 0$, $u_{\max} = 0$.
4. For all x_i do:
   a. Calculate $\varepsilon_i = x_i - y$ (Equation 5).
   b. Calculate $u(\varepsilon_i)$ from Equation 7.
   c. If $\zeta(\varepsilon_i) < k$ ($k = 2$) continue with next x_i (Step 4).
   d. Else calculate the lower bound u_{ex} for the extra uncertainty based on Equation 8. If $u_{\max} < u_{\mathrm{ex}}$ set $u_{\max} = u_{\mathrm{ex}}$ and continue with next x_i (Step 4).
5. If $u_{\max} \neq 0$ then set $u(\delta x) = u(\delta x) + u_{\max}$, set $u_{\max} = 0$ and go to Step 4.
6. If $u_{\max} = 0$ then the data is consistent. Calculate the final uncertainty from Equation 2 and terminate.

We suggest the following principles for combining the data: take the arithmetic or weighted mean and calculate the ζ-values of the difference between the individual data and the mean value and compare it with k (usually k can be set to 2.0); add an uncertainty component to all data values in case any inconsistency is observed (the modified evaluation should be consistent); and propagate the uncertainty as specified in the GUM. This method allows us to use averaging in any stage of the evaluation, and handle the uncertainty correctly.

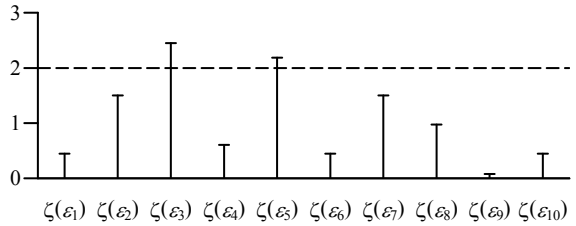

Figure 1: ζ-values for an example data set. The data is considered inconsistent if any ζ-value is larger than 2.0 (ε_3 and ε_5).

References

BIPM, 1993: Guide to the Expression of Uncertainty in Measurement (GUM), ISBN 92-67-1011889, 1st Edition.

Datla R. U., R. Kessel, A. W. Smith, R. N. Kacker and D. B. Pollock, 2009: Uncertainty analysis of remote sensing optical sensor data – Guiding principles to achieve metrological consistency, DOI 10.1080/01431160902897882, *International Journal of Remote Sensing*, **in press**.

Draper, N. R. and H. Smith, 1981: Applied Regression Analysis, Second edition, New York, John Wiley, Section 9.4 page 432.

[by Dr. R. Kessel (NIST)]

Common Reference Value for TOA Total Solar Irradiance

The Common Reference Value (CRV) is the combined value in the time series of data from independent sensors measuring the same quantity. In a recent article that is to appear in the *Journal of Remote Sensing* (Datla *et al.* **in press**), we addressed the problem of how to combine the top of the atmosphere (TOA) Total Solar Irradiance (TSI) time series data currently measured from space. The data from the sensors currently in space – Active Cavity Radiometer Irradiance Monitor III (ACRIM III) on the ACRIM SATellite (ACRIMSAT), the Total Irradiance Monitor (TIM) on the SOlar Radiation and Climate Experiment (SORCE), and the DIfferential Absolute RADiometer (DIARAD) and Physikalisch-Meteorologisches Observatorium (PMO) 6V (PMO6V) on the Solar and Heleospheric Observatory (SOHO) – differ from each other more than their individual quoted uncertainties These sensors are intrinsically SI-traceable standards because of their design and careful construction as electrical substitution radiometers. As an illustration, Figure 1 shows the data from these four sensors for the period from 2003 to 2007.

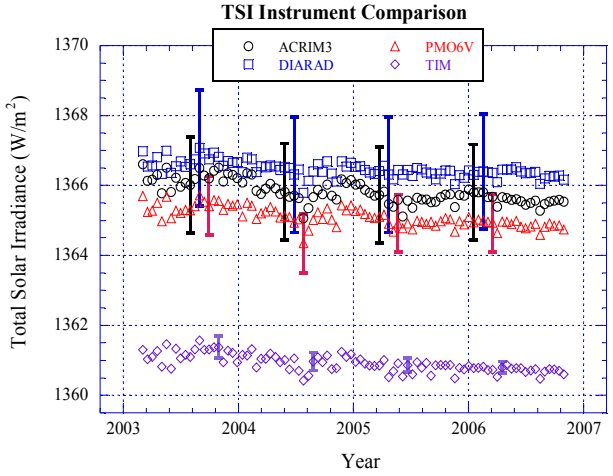

Figure 1: Available TSI data plotted for the overlapping time series of 2003 to 2007 from four satellite sensors. Uncertainty bars represent the combined standard uncertainty for each sensor.

Following the methodology already described by Rüdiger Kessel in this newsletter for application to GSICS inter-comparisons, we determined the CRV time series and associated uncertainty for the data in Figure 1. Based on this analysis the current state of knowledge shows that from 2003 to 2007 the solar irradiance shows a steady decrease from 1365 W/m^2 (units correction) to 1364 W/m^2 in the absolute value. Figure 2 shows a plot of the CRV time series with its k=2 uncertainty bands.

This systematic evaluation of data gives a CRV for TOA/TSI based on the current state of knowledge with uncertainties propagated according to the rules laid out by the ISO Guide to the Expression of Uncertainty in Measurement (GUM) (ISO 1995). However, it should be noted that the CRV and its uncertainty is a dynamic quantity. Our procedure allows the CRV to be updated systematically as new research reveals any corrections to the current sensor data, and improved future

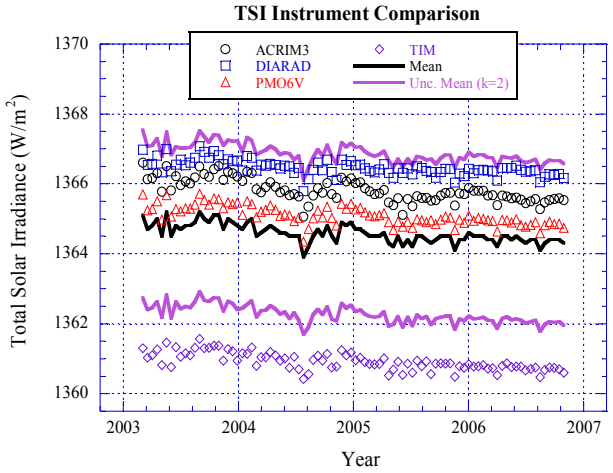

Figure 2: The CRV for the time series after adding an additional uncertainty for each sensor to make the data consistent. Symbols are the data collected for a given instrument. The solid lines represent the arithmetic mean and its expanded uncertainty (k=2).

sensor data adds to the knowledge base. An effort to report the evolving knowledge base, and provide the current evaluation of CRV time series for TOA/TSI through WEB, is underway at NIST.

References

R. U. Datla, R. U., R. Kessel, A. W. Smith, R. N. Kacker and D. B. Pollock, 2009: "Uncertainty analysis of remote sensing optical sensor data – Guiding principles to achieve metrological consistency", International J. of Remote Sensing (http://www.informaworld.com/tres. (**in press**))

International Organization for Standardization, 1995: ISO *Guide to the Expression of Uncertainty in Measurement.* 2nd edn.

[by Dr. R. Datla (NIST)]

Quantifying the Impact of Scene Variability on Inter-Calibration

Inter-calibrations of satellite instruments often require collocation of observations from different instruments. As these procedures are rarely exact, thresholds are usually applied to define the collocations. The choice of these thresholds directly impacts the uncertainty of the comparison, partially due to the scene variability within the range of the collocation criteria.

Scene variability can be quantified by evaluating the root mean square difference of a series of observations sampled at different intervals in space or time. This is similar to the concept of *Structure Functions* in meteorology [Kitchen, 1989] and *Allan Variance* [Allan, 1966]. It allows the variability of stochastic processes to be quantified over specific spatial or temporal scales.

Temporal Variability

The root mean square difference (*RMSD*) is calculated between brightness temperatures, T_bs, sampled at different intervals, Δt, from an extended time-series, $T_b(t)$:

$$RMSD_t(\Delta t) = \left\langle \left[T_b(t+\Delta t) - T_b(t)\right]^2 \right\rangle^{1/2} \qquad (1)$$

Here, the T_b variability is estimated from observations from the infrared channels of the Meteosat-8 SEVIRI imager, which provides data sampled every 3 km at nadir, and every 15 min in normal operations over the full Earth disc (or every 5 min over a limited area). The red curve in Figure 1 shows the results for the 10.8 µm channel on temporal scales of 5 min to 16 hr.

The temporal T_b variability was calculated as *RMSD* from a series of observations, made in rapid scanning mode on 18 Apr 2008, that sampled the area with the latitude segments 15°N 30°W-30°E, 45°N 45°W-45°E, every 5 min over a 24 hr period. The results are consistent with those calculated from a larger area (within 30° lat/lon of the sub-satellite point) scanned every 15 min over another 24 hr period (4 Feb 2006).

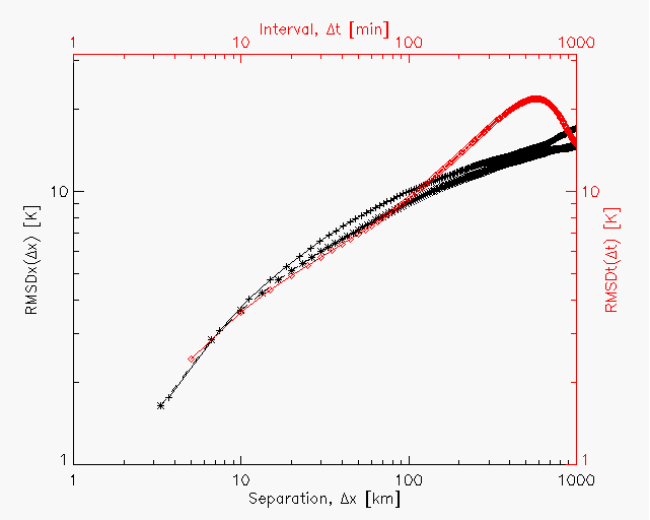

Figure 1: R.M.S. differences in Meteosat-8 10.8 μm brightness temperatures with time intervals from Rapid Scanning Meteosat data (red diamonds) and with spatial separation in North-South direction (black pluses) and West-East direction (black red stars).

$RMSD_t$ in Figure 1 shows most variability for $\Delta t \sim 12$ hr, corresponding to the diurnal cycle. This is common to all channels, but most pronounced in the window channels. It is apparent that the diurnal cycle dominates variability on time scales longer than ~1 hr, causing $RMSD_t$ to increase more rapidly for increasing time intervals.

Spatial Variability

The spatial T_b variability was calculated over the area within 30° lat/lon of the sub-satellite point from data obtained at 01:00 UTC on 1 Feb 2006. The image in each channel was shifted by variable distances, Δx, and the RMSD was calculated for each:

$$RMSD_x = \left\langle \left[T_b(x+\Delta x) - T_b(x) \right]^2 \right\rangle^{1/2} \qquad (2)$$

As expected, the black curves in Figure 1 show $RMSD_x$ increases with increasing spatial separation at scales of 3 to 1000 km. There is more T_b variability in the N/S direction than E/W because of the global latitudinal temperature gradient. However, this difference becomes negligible on scales smaller than ~10 km.

Space-Time Continuum

This figure allows the scene variability to be quantified for observations sampled at any interval in space or time. For example, Table 1 shows the spatial and temporal variability evaluated as the r.m.s. difference in scene T_bs sampled every 3.5 km and 5 min, respectively. For all channels, $RMSD_t(\Delta t$=5min) and $RMSD_x(\Delta x$=3.5km) were found to produce similar variances. So using the observed spatial variability alone will tend to underestimate the uncertainty in each collocation by a factor of $\sim\sqrt{2}$, due to neglecting the temporal variability. In Table 1, the window channels show most variability on these scales, because they are most sensitive to clouds, while the channels more sensitive to atmospheric absorption show least variability.

Table 1: Temporal and spatial variability of Meteosat brightness temperatures on scales of 5 min and 3.5 km, respectively.

Channel [μm]	$RMSD_t(\Delta t$=5min) [K]	$RMSD_x(\Delta x$=3.5km) [K]
3.9	1.7	2.1
6.2	0.4	0.5
7.3	0.8	0.8
8.7	1.7	1.6
9.7	0.9	1.2
10.8	1.8	1.7
12.0	1.8	1.6
13.4	1.2	1.2

Filtering

A homogeneity filter can be applied by excluding pixels where the standard deviation of radiances within 5x5 pixels are >5% of the mean radiance. When this is applied prior to the calculation, $RMSD_t$ drops by a factor of 2.0 and $RMSD_x$ reduces by a factor of 2.6. Selecting only clear sky cases will further reduce both $RMSD_t$ and $RMSD_x$. On very small scales, or for homogeneous scenes, the atmospheric variability will become negligible compared to the instrument's radiometric noise and RMSD will become constant with time and space.

Conclusions

In this study, optimization of collocation thresholds is found to depend on how much noise is acceptable to introduce into each collocation due to scene variability. For example, these results suggest thresholds of 5 min and 3.5 km would each introduce errors of about 1-2 K into each collocation. These may be reduced to insignificant levels if many independent collocations are combined in the analysis. However, adjacent collocations are highly correlated (autocorrelation 1/e scales are about 600 km and 6 hr), so it is not trivial to optimise the collocation thresholds from this analysis alone.

References

Allan, D.W., 1996: "Statistics of Atomic Frequency Standard", *Proc IEEE*, 54, No.2, pp.221-231.

Kitchen, M., 1989: "Representativeness errors for radiosonde observations", *Q.J.R. Meteorol. Soc.*, Vol.115, pp.673-700.

[by Dr. T. J. Hewison (EUMETSAT)]

Inferring NOAA-14 MSU Ch 2 and NOAA-15 AMSU-A Ch 5 Relative Measurement Errors

When comparing data from matched *NOAA-14* (*N14)* Microwave Sounding Unit (MSU) and *N15* Advanced MSU Series-A (AMSU-A) instrument channels using the simultaneous nadir overpass (SNO) method, systematic brightness temperature, T_b, errors (δT_b) due to subtle channel frequency differences can arise. These systematic T_b errors need to be estimated and subtracted from the observed SNO-deduced T_b differences in order to better isolate the systematic error component related to calibration. In this study, δT_b due to subtle frequency center and bandwidth differences between MSU Ch 2 (53.74 GHz) and AMSU-A Ch 5 (53.596 ± 0.115 GHz) are estimated by simulating their T_b values at all near-nadir AMSU-A footprint locations for the 14th or 15th day of each month in 2007. The Microwave Integrated Retrieval System (MIRS) from NOAA, based on the Community Radiative Transfer Model (CRTM) and initialized by the Global Data Assimilation System (GDAS), has been used for this purpose.

In Figure 1, SNO inter-comparison of *N14* MSU Ch 2 and *N15* AMSU-A Ch 5 data before removal of frequency-difference related δT_b are shown for the Northern Hemisphere (NH) and Southern Hemisphere (SH). These figures reveal mainly hemispheric-dependent δT_b that can be larger than 1 K. When CRTM-estimated δT_b related to frequency mismatches are subtracted from the SNO-deduced systematic T_b errors, these hemispheric-dependent δT_b become about 0.11 ± 0.09 K for the NH and -0.07 ± 0.08 K for the SH (see Figure 2).

The MIRS-adjusted SNO-inferred δT_b have been compared with *N14* MSU Ch 2 scene T_b at the SNO events. Also, these T_b systematic errors have been examined for their correlation with instrument parameters related to calibration – e.g., space counts, blackbody counts, as well as local oscillator, platinum resistance thermometer, rf-shelf, and scan motor temperatures – and their differences. The outcome of these statistics showed correlations of less the 0.3 in most cases.

The results presented in this study represent progress in establishing fundamental climate data records from combined MSU/AMSU-A data. On the other hand, the uncertainties related to removing the frequency-difference related δT_b are not fully definable, since systematic errors of the GDAS soundings and surface emissivity inputs to the CRTM model can not be fully resolved. Furthermore, MSU/AMSU-A δT_b related to diurnal cycle differences and changes resulting from inter-satellite orbit differences and drifts, respectively, need to be estimated using a climate model (Mears, 2003) or other means. Some researchers, such as Zou et al. (2006), have neglected this step when establishing MSU-only time series over ocean, where the diurnal cycle is very small.

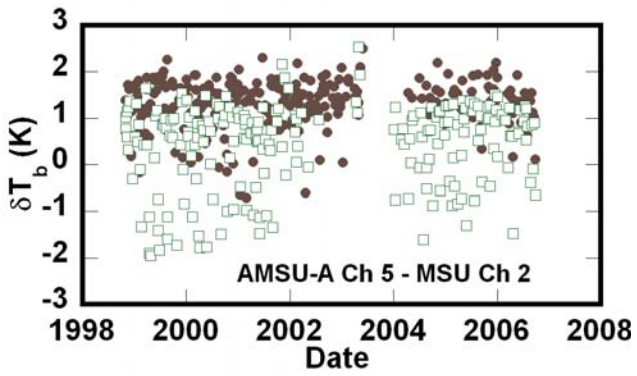

Figure 1: Time series of SNO-estimated δT_b between *N14* MSU Ch 2 and *N15* AMSU-A Ch 5. Northern (Southern) Hemisphere results are denoted by the brown dots (green squares).

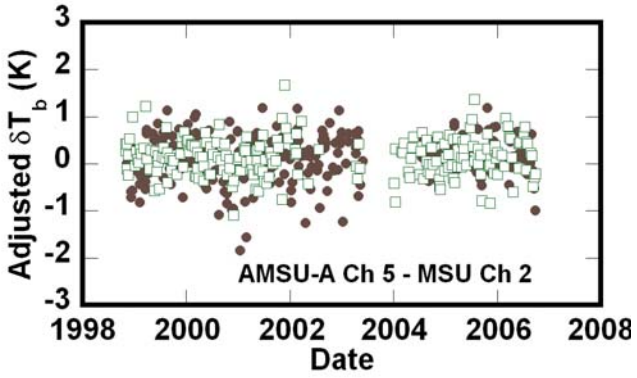

Figure 2: Time series of SNO-estimated δT_b between *N14* MSU and *N15* AMSU-A that have been adjusted for frequency-difference related T_b biases using NOAA MIRS. Northern (Southern) Hemisphere results are denoted by the brown dots (green squares).

After net calibration and diurnal δT_b have been estimated between *N14* MSU Ch 2 and *N15* AMSU-A Ch 5, the total T_b systematic errors between sensor units must be consecutively and cumulatively removed between each successive instrument pair from the first MSU satellite in the time series to the last AMSU-A satellite.

References

Iacovazzi, R. A., Jr., C. Cao, and S. Boukabara (2009), Analysis of Polar-orbiting Operational Environmental Satellite NOAA-14 MSU and NOAA-15 AMSU-A relative measurement biases for climate change detection, *J. Geophys. Res.*, 114, D09107, doi:10.1029/2008JD011588.

C. A. Mears, M. Schabel, and F. J. Wentz, 2003: A reanalysis of the MSU Channel 2 tropospheric temperature record. *J. Climate*, **16**, 3650-3664.

Zou, C.-Z., M. D. Goldberg, Z. Cheng, N. C. Grody, J. T. Sullivan, C. Cao, and D. Tarpley, 2006: Recalibration of Microwave Sounding Unit for climate studies using simultaneous nadir overpasses. *J. Geophys. Res.*, **111**, D19114, doi:10.1029/2005JD006798.

[by Drs. R. Iacovazzi, Jr., C. Cao, and S.-A. Boukabara (NOAA)]

News in this Quarter

Summary of the Joint GRWG-IV and GDWG-III Meeting

The GSICS Research Working Group (GRWG) and Data Working Group (GDWG) met 28-30 January 2009 in Tokyo, Japan. The Japan Meteorological Agency (JMA) hosted the meeting at its headquarters. Drs. Volker Gärtner and Fred Wu, chair of GDWG and GRWG, respectively, co-chaired the meeting. Yoshiro Kozawa, Director-General of JMA Observations Department, welcomed the delegates at the beginning of the meeting. Tetsu Hiraki, Director-General of JMA, hosted a reception for the meeting in the evening. Meeting participants were very appreciative of JMA for logistical support and hospitality.

Attending the meeting (Fig. 1) were 24 delegates and 6 observers from 15 government agencies, universities, and inter-government organizations. These include Chiba University, China Meteorological Administration (CMA), Centre National d'Etudes Spatiales (CNES), European Organisation for the Exploitation of Meteorological Satellites (EUMETSAT), Japan Aerospace Exploration Agency (JAXA), JMA, Korea Meteorological Administration (KMA), National Aeronautics and Space Administration (NASA), NOAA, Seoul National University, University of Tokyo, University of Wisconsin (by telephone), Utah State University, and World Meteorological Organization (WMO). The meeting was composed of a two-day joint session for review and discussion of issues of mutual interest to both working groups, with a one-day break-out session in between.

Figure 1: Joint GRWG-IV and GDWG-III Meeting group picture.

In the joint session, administrative briefings were given by the GSICS Executive Panel WMO representative, GRWG and GDWG chairs, and the GSICS Coordination Center (GCC) deputy director. Meanwhile, progress reports were given by representatives of GSICS Processing and Research Centers (GPRCs), including, EUMETSAT, NOAA, JMA, KMA, and CMA; and by T. Hewison on the hierarchical structure for the Algorithm Theoretical Basis Document (ATBD) as the framework for GSICS. Participants were pleased with the progress. In particular, all GPRCs are now capable of generating some GSICS products, and some of the GSICS activities have led to positive impact on satellite operations.

Other presentations and discussions held during the joint sessions include Dr. D. Tobin's briefing on the sampling strategy of the planned Climate Absolute Radiance and Refractivity Observatory (CLARREO), and its impact on inter-calibration. Participants recognized the importance of CLARREO to obtain SI-traceable measurements from space, which is especially valuable to GSICS. The ability of GSICS users to use ground reference data from the SADE data base was introduced by D. Blumstein. Participants also had a vigorous discussion regarding GSICS products. In this discussion, the consensus was that the initial GSICS core product should be the inter-satellite "GSICS Correction", which would be a function depending on satellite, channel, time, location, and other factors, and would be well characterized in terms of uncertainty. Other presentations were made regarding the GSICS Procedure for Product Acceptance, GSICS web meetings using Centra, and the GSICS Wiki. Furthermore, a GSICS Users Workshop is planned in conjunction with the September 2009 EUMETSAT Satellite Meteorology Conference in Bath, UK.

The purpose of the GDWG breakout meeting was to review specific data management issues. Amongst them was the GSICS web presence and GSICS collaboration server issues. Furthermore it was intended to identify the work achievable by the GDWG for the next months. Specifically, the group discussed the following items: creation of a GSICS central website; review of the GCC and GPRC web sites; creation of a GSICS portal; harmonisation of GSICS product presentation; provision of calibration data from the CNES SADE database; and operational issues for the GSICS collaboration servers.

In the GRWG breakout meeting, status reports were given by CMA, EUMETSAT, JMA, KMA, NASA, and NOAA. Topics covered in these presentations include visible and infrared instrument inter-comparison and vicarious calibration. Also discussed were the Committee on Earth Observation Satellites (CEOS) Working Group on Calibration/Validation (WGCV) Quality Assurance for Earth Observations (QA4EO) review, and the 2009 Operation Plan.

Near the close of the meeting, both groups discussed and introduced new action items to be carried out in the next year. The agenda, minutes, and presentations from the Joint GRWG-IV and GDWG-III meeting can be accessed by following the "Meeting reports" menu item link at the GSICS central website: http://gsics.wmo.int or the GCC web site. A tentative location for the next Joint GRWG and GDWG meeting was set for early in 2010 in Toulouse, France to be hosted by CNES.

[by R. Iacovazzi (NOAA) and J. Lafeuille (WMO)]

Current status of COMS satellite

Korea Meteorological Administration (KMA) has started its first Korean multi-purpose geostationary satellite program named Communication, Ocean and Meteorological Satellite (COMS), in cooperation with three other government ministries since 2003. Multi-missions of COMS are intended

not only for meteorological and oceanic observations for public welfare, but also for in-orbit tests of the developed communication payload to be used for the next geosynchronous satellite.

The Korea Aerospace Research Institute (KARI) has been developing COMS for KMA. COMS will be a three-axis stabilised multi-purpose satellite. Table 1 presents the planning details as known so far.

Table 1. Chronology of the COMS programme

Satellite	Launch	End of service	Position	Status (Aug 2007)	Instruments
COMS 1	2009	Expected ≥ 2016	128.2°E	Being defined	Meteorological imager (MI), Geostationary Ocean Color Imager (GOCI)
COMS 2	2016	Expected ≥ 2023	116.2°E /128.2°E (TBD)	Being defined	(TBD)

The COMS payload for earth observation includes a Meteorological Imager (MI) and a Geostationary Ocean Color Imager (GOCI). The MI has five channels (see Table 2) in the range 0.55-12.5μm. The resolution of these channels is 1 km in the VIS channel, and 4 km in four IR channels. A full disk image is captured every 27 min (proportionally less for limited areas).

Table 2. COMS MI channel specifications.

Central Wavelength	Spectral Interval	Radiometric accuracy (NEΔT or SNR)
0.675 μm	0.55 - 0.8 μm	10:1@5% albedo, 170:1@ 100 % albedo
3.75 μm	3.50 - 4.0 μm	0.10 K @ 300 K
6.75 μm	6.5 – 7.0 μm	0.12 K @ 300 K
10.8 μm	10.3 – 11.3 μm	0.12 K @ 300 K
12.0 μm	11.5 – 12.5 μm	0.20 K @ 300 K

Meanwhile, GOCI has eight narrow-band channels in the range 400-865 nm for ocean color monitoring (see Table 3),

Table 3. COMS GOCI channel specifications.

Central Wavelength	Band Width	Radiometric Accuracy (SNR @ Specified input radiances)
412 nm	20 nm	1000 @ 0.100 W m^{-2} sr^{-1} μ^{-1}
443 nm	20 nm	1090 @ 0.086 W m^{-2} sr^{-1} μ^{-1}
490 nm	20 nm	1170 @ 0.067 W m^{-2} sr^{-1} μ^{-1}
555 nm	20 nm	1070 @ 0.056 W m^{-2} sr^{-1} μ^{-1}
660 nm	20 nm	1010 @ 0.032 W m^{-2} sr^{-1} μ^{-1}
680 nm	10 nm	870 @ 0.031 W m^{-2} sr^{-1} μ^{-1}
745 nm	20 nm	860 @ 0.020 W m^{-2} sr^{-1} μ^{-1}
865 nm	40 nm	750 @ 0.016 W m^{-2} sr^{-1} μ^{-1}

and a resolution of 500 m over a limited coverage (2500 km × 2500 km).

Raw data transmission from COMS are transmitted to: Korea Meteorological Satellite Center (KMSC/KMA); Korea Ocean Satellite Center (KOSC); and the Satellite Operation Center. This transmission has a frequency of 1687 MHz, bandwidth of 6.0 MHz, RHCP/LHCP polarisation, and 6 Mbps data rate.

After ground processing at MSC and/or KOSC, data are re-transmitted to the users by:

- HRIT (High Rate Information Transmission)
  - Frequencies of 1695.4 MHz; bandwidth of 5.2 MHz; and Linear Polarization in horizontal direction
  - Antennas: diameters of 3.7 m; G/T ~ 11.1 dB/K; and 3 Mbps data rate
- LRIT (Low Rate Information Transmission)
  - Frequencies of 1692.14 MHz; bandwidth of 1 MHz; and Linear Polarization in horizontal direction
  - Antennas: diameters of 1.2 m(down), G/T ~ 1.9 dB/K, and 256 kbps data rate.

The status of COMS is that the Critical Design Review (CDR) of the COMS spacecraft was completed in March 2007, and the Assembly, Integration, and Test (AI&T) began in September 2007. The integration of MI and GOCI to the spacecraft occurred at the end of 2008, and the compatibility test of the whole COMS system was performed until the first quarter of 2009. COMS is scheduled to be launched in fourth quarter of 2009, followed by six month's In-Orbit Test in order to confirm the performance of the satellite system.

[by Dr. D. Kim (KMA)]

Just Around the Bend …

GSICS-Related Meetings

- **SPIE Optics and Photonics,** 2-6 August 2009, San Diego, CA, USA, http://spie.org/optics-photonics.xml.
- **CALCON Technical Conference,** 24-27 August 2009, Logan, UT, USA, http://www.sdl.usu.edu/conferences/calcon/.

GSICS Publications

Iacovazzi, R. A., Jr., C. Cao, and S. Boukabara (2009), Analysis of Polar-orbiting Operational Environmental Satellite NOAA-14 MSU and NOAA-15 AMSU-A relative measurement biases for climate change detection, *J. Geophys. Res.*, 114, D09107, doi:10.1029/2008JD011588.

Tahara, Y. and K. Kato, 2009: New spectral compensation method for inter-calibration using high spectral resolution sounder, Met. Sat. Center Technical Note, No. 52, 1-37. http://mscweb.kishou.go.jp/monitoring/gsics/ir/techinfo.htm.

GSICS Classifieds

Are you looking to establish a GSICS-related collaboration, or do you have GSICS-related internships, exchange programs, and/or available data and services to offer? *GSICS Quarterly* includes a classified advertisements section on an as-needed basis to enhance communication amongst GSICS members and partners. If you wish to place a classified advertisement in the newsletter, please send a two to four sentence advertisement that includes your contact information to Bob.Iacovazzi@noaa.gov.

Acknowledgments:

The *GSICS Quarterly* Editor would like to thank those individuals who contributed articles and information to this newsletter. The Editor would also like to thank *GSICS Quarterly* European Correspondent, Dr. Tim Hewison of EUMETSAT, and Asian Correspondent, Dr. Yuan Li of CMA, in helping to secure articles for publication.

The *GSICS Quarterly* Press Crew is looking for short articles (<1 page), especially related to cal/val capabilities and how they have been used to positively impact weather and climate products. Unsolicited articles are accepted anytime, and will be published in the next available newsletter issue after approval/editing. **Please send articles to Bob.Iacovazzi@noaa.gov, *GSICS Quarterly* Editor.**